2950 Niles Road, St. Joseph, MI 49085-9659, USA
269.429.0300 fax 269.429.3852 hq@asabe.org www.asabe.org

An ASABE Meeting Presentation

Paper Number: 1009114

Hyperspectral Image Analysis for Plant Stress Detection

Yunseop Kim, Research Associate

Appalachian Fruit Research Station, USDA-ARS, 2217 Wiltshire Road, Kearneysville, WV 25430 USA, james.kim@ars.usda.gov

D. Michael Glenn, Plant physiologist

Appalachian Fruit Research Station, USDA-ARS, 2217 Wiltshire Road, Kearneysville, WV 25430 USA, michael.glenn@ars.usda.gov

Johnny Park, Research Assistant Professor

Electrical and Computer Engineering, Purdue University, 465 Northwestern Avenue, West Lafayette, IN 47907 USA, jpark@purdue.edu

Henry K. Ngugi, Assistant Professor

Plant Pathology, Pennsylvania State University, 290 University Drive, Biglerville, PA 17307 USA, hkn3@psu.edu

Brian L. Lehman, Research Technician

Plant Pathology, Pennsylvania State University, 290 University Drive, Biglerville, PA 17307 USA, bll143@psu.edu

Written for presentation at the
2010 ASABE Annual International Meeting
Sponsored by ASABE
David L. Lawrence Convention Center
Pittsburgh, Pennsylvania
June 20 – June 23, 2010

Abstract. *Plant stress significantly reduces plant productivity. Automated on-the-go mapping of plant stress allows for timely intervention and mitigation of the problem before critical thresholds are exceeded, thereby maximizing productivity. A hyperspectral camera analyzed the spectral signature of plant leaves to identify the plant water stress. Five different levels of water treatment were created on young apple trees (Buckeye Gala) in a greenhouse and continuously monitored with a hyperspectral camera along with an active-illuminated spectral vegetation sensor and a digital color camera. Individual spectral images over a 400 – 1000 nm wavelength range were extracted at a specific wavelength to estimate reflectance and generate spectral profiles for five groups of apple*

trees at different water treatment levels. Various spectral indices were investigated and correlated to stress levels. The highest correlation was found with Red Edge NDVI at 705 nm and 750 nm in narrowband indices and NDVI at 680 nm and 800 nm in broadband indices. The experimental results indicate that intelligent optical sensors could deliver decision support for plant stress detection and management.

Keywords. Sensors, illumination, spectral response, measurement, leaves, water stress.

Introduction

Plant stress caused by biotic or abiotic factors that adversely affect plant growth significantly reduces productivity. When a plant becomes stressed, stress is expressed in the plant canopy by many types of symptoms. Water stress, for example, closes stomata and impedes photosynthesis, resulting in changes in leaf color and temperature (Nilsson, 1995). Other stress symptoms include morphological changes such as leaf curling or wilting.

Early detection of plant stress is critical to prevent plants terminal stress and minimize acute and chronic loss of productivity. The severity of damage depends on the duration between onset and time of detection. At the orchard level, the effectiveness of any remedial measures depends on the timely detection and identification of the cause of stress. Human vision is unique and comprehensive, but subject to individual differences in light perception, which drives inconsistency in estimating the color and pattern of plant stress symptoms. Substantial variations in rating visual stress assessment were reported in many studies (Sherwood et al, 1983; Shokes et al, 1987; Weber and Jorg, 1991; Nutter and Schultz, 1995). Fredericksen and Skelly (1994) reported that net photosynthetic rate decreased up to 14% before visible symptoms of ozone injury. Remote sensing technology provides an objective and consistent means of assessing plant stress and has the capability to record important spectral details in longer wavelengths that are beyond a visible range (400 – 700 nm).

Plant leaves absorb the majority of radiance in the visible band by plant pigments such as chlorophyll and xanthophylls, but reflects most radiance in the near-infrared (NIR) band. Plant stress changes the reflectance pattern due to an efficiency drop of photosynthetic absorbance and causes reflectance to increase in the visible band and to decrease in the NIR band. Thus, combining data from spectral bands into indices such as NIR/Red or (NIR-Red)/(NIR+Red) amplifies spectral differences provides additional details for stress detection. The first index NIR/Red, which is called the simple ratio (SR), is often closely correlated to the leaf area index (LAI), whereas the latter index (NIR-Red)/(NIR+Red), or the normalized difference vegetation index (NDVI) is often closely correlated to green biomass (Nilsson, 1995). Other spectral indices used for plant stress detection include the physiological reflectance index (PRI) (Gamon et al., 1997; Suarez et al., 2008) that uses 531 nm and 571 nm for photosynthesis light use efficiency, water index (WI) (Penuelas et al., 1995; Champagne et al., 2001) that uses 900 nm and 970 nm for water absorption feature, and Red Edge NDVI (Gitelson and Merzlyak, 1994; Sims and Gamon, 2002) that uses red edge at 705 nm and 750 nm for changes in vegetation heath.

Stress detection is often difficult and challenging to identify causes, because plant stress can be a compound effect of water, nutrient, disease, and/or insects. Accurate control of healthy and stressed plants isolates irrelevant factors and helps detection focus on a particular stress factor. This paper presents 1) detection of plant water stress using a hyperspectral sensor and 2) performance of an active-illuminated spectral sensor and a digital camera for measuring NDVI values on apple trees.

Materials and Methods

A multimodal sensor system was designed to measure the spectral signature of leaf surfaces and identify plant stress. In its initial design, the multimodal sensor system was equipped with four sensors: two normalized difference vegetation index (NDVI) sensors, a hyperspectral camera, and a digital color camera (**Error! Reference source not found.**). The NDVI sensors scan the middle of the tree canopy at a distance of 100 cm from the canopy, while the two cameras capture images, recording overlapped multi-modal images and spectral data as a vehicle drives along the tree row.

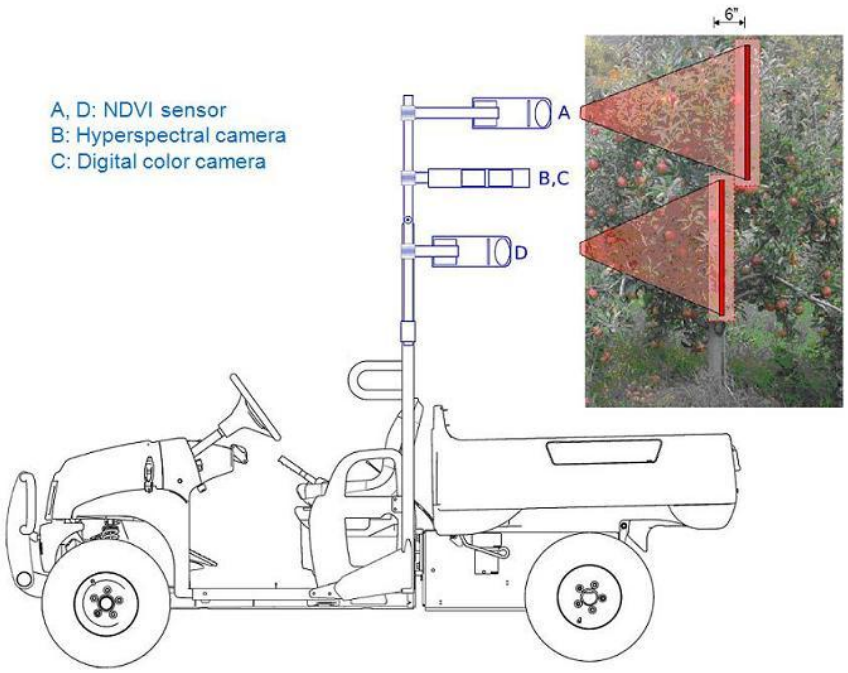

Figure 1. Initial schematic design of a multi-modal sensor system for plant stress detection.

The hyperspectral camera (ImSpector V10E, Spectral Imaging Ltd., Finland) is equipped with a spectral range of 400 – 1,000 nm with 5 nm interval and a 12-bit CCD that produces a 1392 (column/line scan) x 373 (row/mirror's 60^{o} scan) image at 9 frames/sec. The NDVI sensor (GreenSeeker, Ntech Industries, Ukiah, CA) records a single point measurement of NDVI at Red (660 nm ± 12 nm) and NIR (770 nm ± 12 nm) wavebands at 81 – 122 cm standoff distance with 61 cm ± 10 cm line scan width. The digital camera (Dragonfly 2, Point Grey, Canada) is equipped with a 1024 x 768 color CCD. The system also uses two light sensors (Silicon and 3-sensor quantum bar, Spectrum Technologies Inc., Plainfield, IL) to record the amount of radiation from a light source. The Silicone captures solar radiation at 300 – 1,100 nm, while the quantum bar measures the radiation at 400 – 700 nm.

Multi-modal data acquisition (MMDAQ) software was developed to integrate the multi-modal sensors and interface data communication: FireWire for the digital camera and RS232 serial for the NDVI sensors. An initial design of the MMDAQ software was completed with three graphical user interface (GUI) dialog windows: Digital Camera Capture View, Segmentation, and NDVI Sensor (**Error! Reference source not found.**). A color image is acquired by a SNAP button with selection of RGB (or one of R, G, and B buttons for a monocular image). An AUTO SNAP button automatically saves images at a fixed interval. The captured or retrieved image is segmented by threshold values that are manually selected and preset in the R, G, and B channels individually with the display of a histogram distribution. NDVI sensor data is acquired by a "READ" button and displayed at 10 readings/sec and saved to a file with a time stamp.

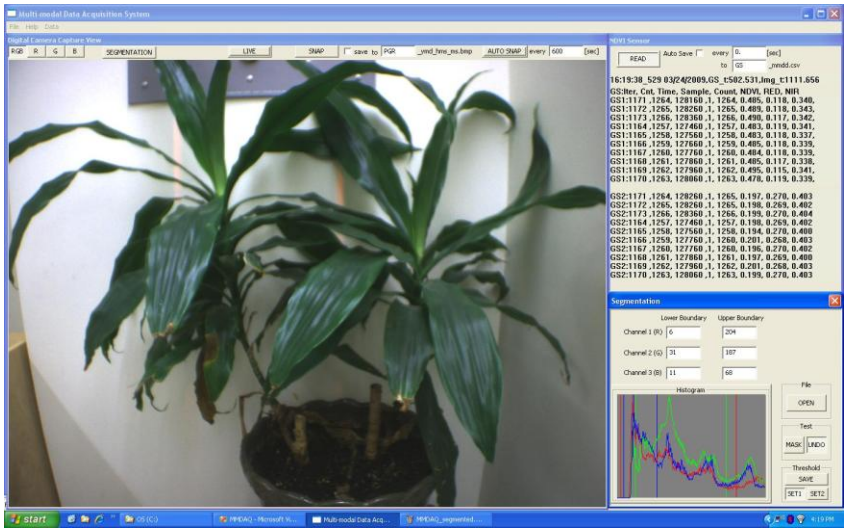

Figure 2. Multi-modal data acquisition (MMDAQ) software with GUI dialog windows of Digital Camera Capture View, Segmentation, and NDVI Sensors.

Greenhouse experiments for plant water stress detection were carried out at the Pennsylvania State University (PSU) - Fruit Research and Extension Center (FREC) in Biglerville, PA during the growing season of 2009. The main goal of the experiments was to capture morphological and spectral features of trees at different levels of water stress. Twenty apple (cv. 'Buckeye Gala') trees grafted on ELMA 26 rootstocks and potted in Berger BM1 potting medium were used for the water stress study. The trees were watered regularly by drip irrigation and sprayed at 7-10 day interval to control mites, insects, and powdery mildew.

The multi-modal sensor system was mounted on a cart with extended support pipes and positioned to get a nadir view over the top of canopies (Fig. 3). A mounting frame holds two NDVI sensors that are horizontally staggered to scan a vertical FOV, while another frame holds two tripod heads attached to the hyperspectral camera and digital camera. Data collection was carried out on five groups of apple trees at different water treatment levels (100%, 90%, 75%, 60%, and 45% at field capacity) with four replications per group and continued on a weekly basis from late April to June. Water treatment levels were defined as the percentage replacement of water content to bring the tree to field capacity and were measured by weighing the containers before irrigation in order to calculate the needed replacement amount.

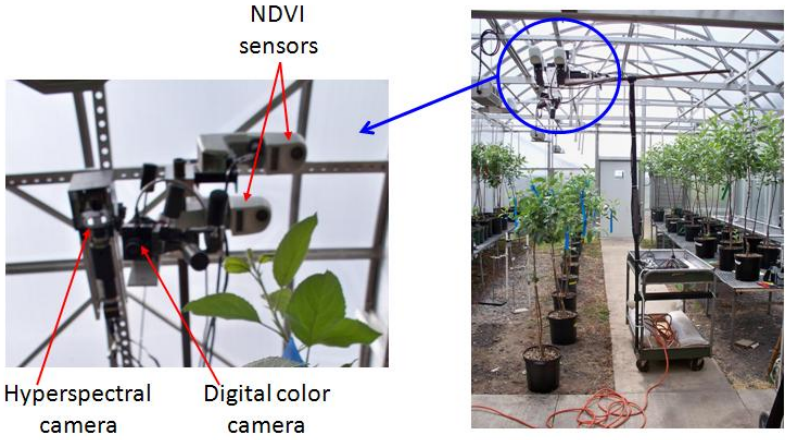

Figure 3. Greenhouse experimental setup with 20 apple trees in five different groups of water treatments for water stress detection.

The hyperspectral camera generates a set of images or a cube image, $R_j(i,k)$ where i is the horizontal spatial resolution, k the spectral resolution, and j the vertical spatial resolution created by a mirror rotation (373/60^o full scan). A spectral cube image is first calibrated with dark and white reference images prior to image acquisition. Dark reference images, $D_j(i,k)$ were acquired by covering the lens with a dark cloth, while white reference images, $W_j(i,k)$ were acquired by placing a white board in front of the lens under ambient illumination. Each reference image was obtained by averaging measurements from 30 images, $D_{ave}(i,k)$ (Eqn. (1)) and $W_{ave}(i,k)$ (Eqn. (2)). Differences of white and dark reference images are subtracted by the minimum value of the differences and divided by the maximum value of the differences, generating a normalized range of pixel distribution, $N_{ave}(i,k)$ (Eqn. (3)). When a new raw image, $R_j(i,k)$ is acquired, in the same way, difference of raw and dark reference images is subtracted by the minimum value of the difference to trim out dark current noises. The resulting pixel values are then divided by the normalized pixel range to generate a calibrated image, $C_j(i,k)$ (Eqn. (4)).

$$D_{ave}(i,k) = \frac{1}{30}\sum_{j=1}^{30} D_j(i,k) \quad (1)$$

$$W_{ave}(i,k) = \frac{1}{30}\sum_{j=1}^{30} W_j(i,k) \quad (2)$$

$$N_{ave}(i,k) = \frac{[W_{ave}(i,k) - D_{ave}(i,k)] - \min[W_{ave}(i,k) - D_{ave}(i,k)]}{\max[W_{ave}(i,k) - D_{ave}(i,k)]} \quad (3)$$

$$C_j(i,k) = \frac{[R_j(i,k) - D_{ave}(i,k)] - \min[R_j(i,k) - D_{ave}(i,k)]}{N_{ave}(i,k)} \quad (4)$$

The hyperspectral images were further processed to calculate plant stress indices. Thirteen different spectral indices that have been published previously (Table 1) were evaluated for plant stress detection. The seventeen individual spectral images needed for the spectral index calculations were extracted, and the vegetation area in each image was segmented using the corresponding NDVI image and processed to calculate canopy reflectance. Hyperspectral images were collected along with NDVI sensor measurements and color images.

Table 1. Spectral indices that were evaluated for plant stress detection. The three digit numbers following the letter *R* in each formula represent the response of the hyperspectral camera at that particular wavelength.

Broadband Greenness	NDVI (Normalized Difference Vegetation Index)	$= \frac{R800 - R680}{R800 + R680}$
	SRI (Simple Ratio Index)	$= \frac{R900}{R680}$
	EVI (Enhanced Vegetation Index)	$= 2.5 \times \frac{R800 - R680}{R800 + 6 \times R680 - 7.5 \times R450 + 1}$
	ARVI (Atmospherically Resistant Vegetation Index)	$= \frac{R800 - (2 \times R680 - R450)}{R800 + (2 \times R680 - R450)}$
Narrowband Greenness	Red Edge NDVI	$= \frac{R750 - R705}{R750 + R705}$
	Modified Red Edge NDVI	$= \frac{R750 - R705}{R750 + R705 - 2 \times R445}$

	Modified Red Edge SRI	$= \frac{R750 - R445}{R705 - R445}$
	VOG REI (Vogelmann Red Edge Index) 1	$= \frac{R740}{R720}$
	VOG REI 2	$= \frac{R734 - R747}{R715 + R726}$
	VOG REI 3	$= \frac{R734 - R747}{R715 + R720}$
Light Use Efficiency	PRI (Photochemical Reflectance Index)	$= \frac{R531 - R570}{R531 + R570}$
Dry or Senescent Carbon	PSRI (Plant Senescence Reflectance Index)	$= \frac{R680 - R500}{R750}$
Canopy Water Content	WI (Water Index)	$= \frac{R900}{R970}$

Results

Hyperspectral Image Analysis

Spectral image responses are plotted in Fig. 4 over the entire spectral wavelengths (400 – 1000 nm). The spectral profile corresponding to the healthy tree group (100%) follows a typical spectral signature of plant leaves: a small peak at the green band (550 nm), a small drop at the red band (650 nm), and a rising plateau at the near-infrared (NIR) band (750 – 1000 nm). Two groups of water treatments, 90% and 75%, show a trend similar to that of the non-stressed 'healthy' tree group (100%), whereas the spectral profiles corresponding to the 60% and 45% water treatments show an increase of reflectance in the green and red bands and a decrease in the NIR band in comparison with healthy plants.

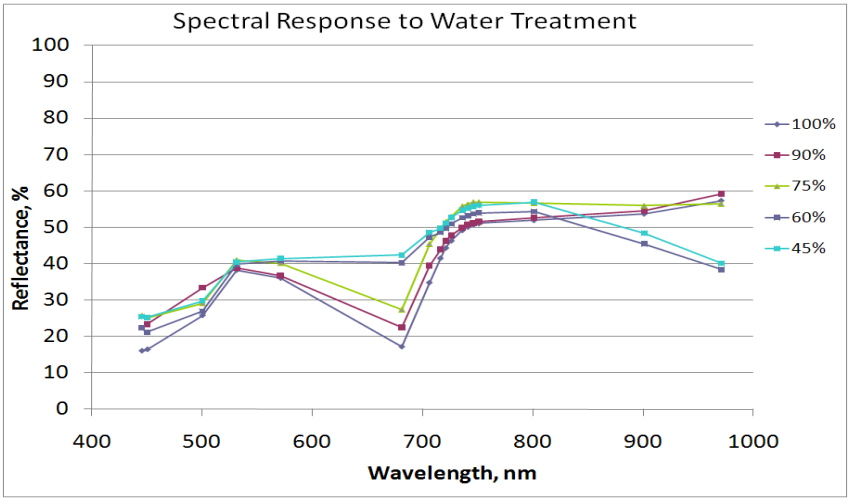

Figure 4. Spectral image response of apple trees subjected to different levels moisture stress by water denial.

Spectral reflectance values in the red band were about 15% higher than typical spectrum of control plant leaves due to image formation and sensitivity of the sensor. We noticed the

hyperspectral camera is sensitive to the reference dark and white images during the calibration procedure. Our assumption is that the illumination condition remains the same during the image acquisition until the next calibration. However, the illumination condition as measured by solar radiation varied broadly during most of the measurements as shown in Fig. 5. Based on this observation, the image data that were severely distorted by rapid illumination changes during image acquisition were not included for further analysis.

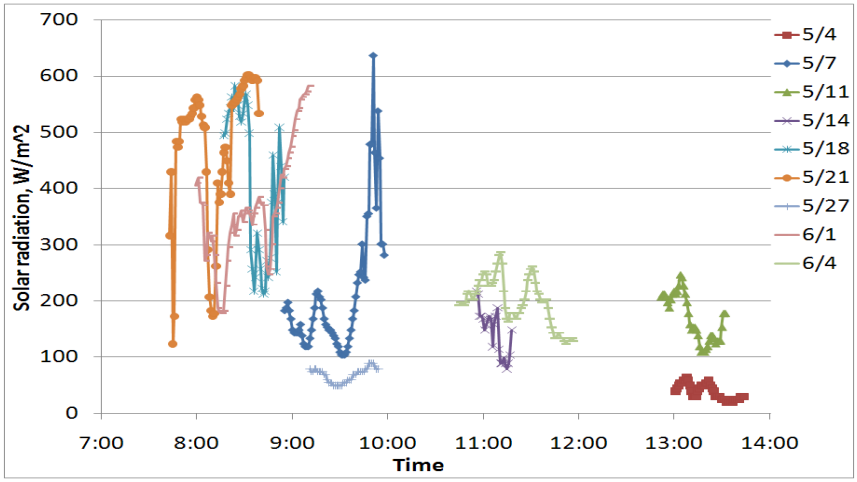

Figure 5. Ambient illumination status recorded during hyperspectral data collection.

Soil water conditions were also monitored every hour continuously from April through June, 2009. Figure 6a shows soil matric potentials and indicates that high potentials (i.e., water stress), occurs on the 60%- and 45%-watered groups. By contrast, the potentials in 100%-, 90%-, and 75%-watered groups remain low mostly under 20 kPa, indicating well watered soil conditions. The repeated peaks in the graph were generated by daily watering based on the water treatment plan. The average daily soil water status of five groups is plotted in Fig. 6b along with dates of hyperspectral image data collection. Higher soil matric potentials at 45%- and 60%-watered groups indicate more water stress. No significant differences were noted in soil water content among the 100%-, 90%- and 75%-watered groups.

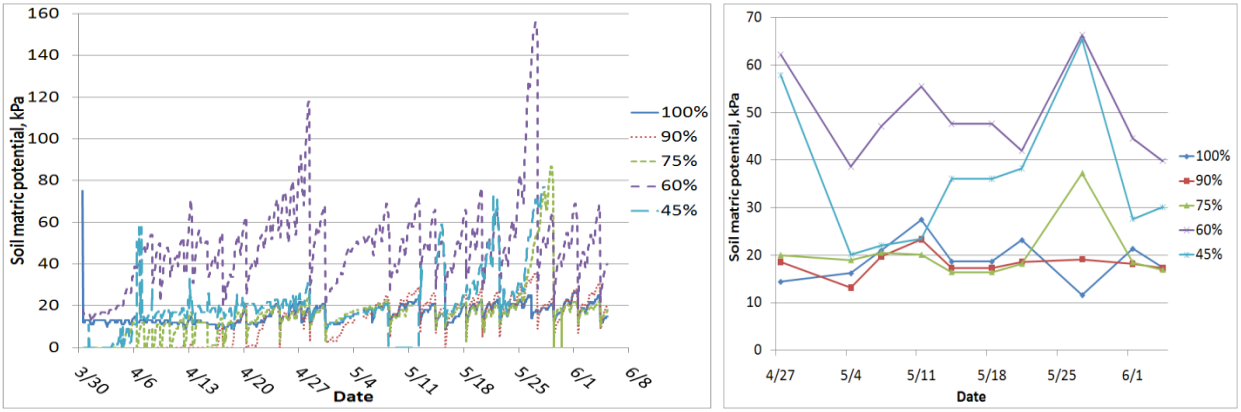

(a) (b)

Figure 6. Soil water status monitored with a Watchdog datalogger and Watermark soil moisture sensor (a) every hour continuously from April – June, 2009, (b) average daily soil water status. Higher soil potentials at 45% and 60% indicate water stressed plants.

The results of four best indices from the images acquired on May 4, 7, 11, and June 4, 2009 are shown in Fig. 7. The highest correlation among narrowband greenness indices was found at Red Edge NDVI with $r^2 = 0.89$ (Fig. 7c). NDVI had the highest correlation among broadband greenness indices with $r^2 = 0.68$ (Fig. 7a). Table 2 presents the correlation coefficients of selected indices to water stress over the tree images. The broadband indices compare a reflectance peak in near infrared (NIR) to another peak in red range where chlorophyll absorbs photons for photosynthesis. Since these features are spectrally broad, they can work effectively with broadband multispectral sensors. The narrowband indices use red edge that is a steeply sloped region of the vegetation reflectance curve between 690 nm and 740 nm, and caused by the transition from chlorophyll absorption to NIR leaf scattering. Since narrowband measurements in the red edge are more sensitive to smaller changes in vegetation health than broadband indices, narrowband indices are suitable for hyperspectral sensors. The result of our experiment with the hyperspectral camera supports this conclusion, resulting in better performance with narrowband indices.

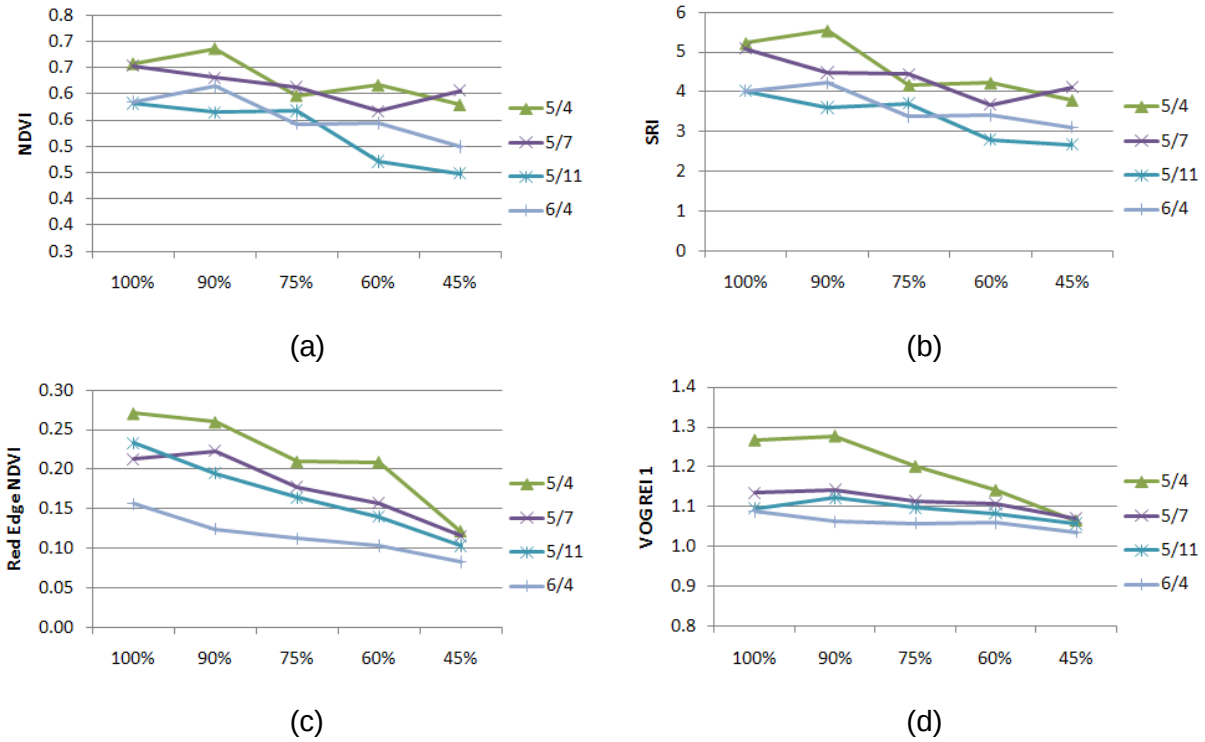

Figure 7. Hyperspectral image responses to water treatments (a) NDVI, (b) SRI, (c) Red Edge NDVI, and (c) VOG REI 1.

Table 2. Correlation coefficients of spectral indices that were evaluated for plant stress detection.

		4/27	5/4	5/7	5/11	6/4	R	R^2
Broadband Greenness	NDVI	0.70	0.83	0.76	0.93	0.89	0.82	0.68
	SR	0.55	0.89	0.81	0.94	0.90	0.82	0.67
Narrowband Greenness	Red Edge NDVI	0.86	0.95	0.96	0.99	0.96	0.94	0.89
	Modified Red Edge NDVI	0.11	0.88	0.91	0.96	0.65	0.70	0.49
	VOG1	0.95	0.98	0.94	0.82	0.89	0.91	0.84
Light Use Efficiency	PRI	1.00	-0.27	-0.02	0.65	0.38	0.35	0.12
Canopy Water	WI	-0.75	0.98	-0.28	0.62	-0.78	-0.04	0.00

Content	PRI*WI	1.00	0.37	-0.03	0.73	0.32	0.48	0.23

NDVI Sensor Analysis

NDVI values of both the vegetation area of tree canopy and the non-vegetation area between trees were obtained with the NDVI sensor. Figure 8a shows continuous readings of NDVI in which higher values are from the vegetation area of canopy and lower values are from the non-vegetation background. NDVI values corresponding to each apple tree were manually selected by comparing a digital image in the same time stamp and marked in circles in Fig. 8a. Average NDVI responses over 13 measurement dates generally match to water treatment patterns with correlation of r = 0.6 (Fig. 8b). Low correlation may be due to measurement errors in the data manually selected from unsynchronized NDVI readings and digital image acquisition.

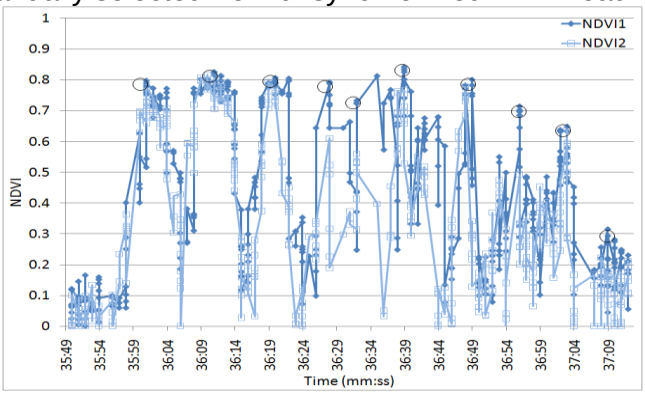

(a)

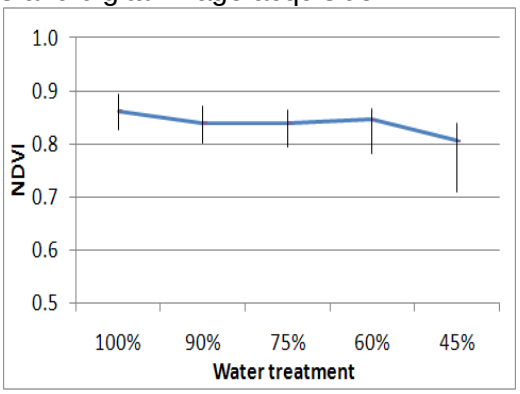

(b)

Figure 8. NDVI sensor responses to water treatments: (a) continuous readings of vegetation of tree canopy and non-vegetation area between trees, (b) average NDVI over 13 measurement dates indicating correlation (r = 0.6) between NDVI measurements and plant water treatment.

Leaf Area Index Analysis

Leaf area index (LAI) provides an important parameter, as leaf area influences photosynthesis and plant growth. A value of LAI = 3 is obtained when almost 100% of the incoming light is intercepted and thus corresponds to a canopy coverage of 100% (Potato Explorer, 2010). Digital images were acquired from nadir view and processed for canopy coverage. Figure 9 displays an image sequence of apple trees with five different water treatments. Images are placed in a chronological order from April 27 to June 18 at an interval of 3 – 5 days. Canopy coverage was calculated by image segmentation of canopy area with NDVI image masking and presented in percentage of canopy coverage. As plants grow over the time, the growth pattern is an increase in the beginning of the time period, followed by a relatively static period of growth in the middle (May 10 – June 10) (Fig. 10a). After June 10, there are clear decreases of canopy coverage in 60%- and 45%-watered groups, while in the other three groups the canopy coverage remains high and static. The average percentage canopy coverage over the period shows 50% in 100%-watered trees and 27% in 45%-watered trees (Fig. 10b), resulting in overall correlation of r = 0.7. The result indicates that canopy coverage measurement can be used as a supplemental index of chronic plant water stress.

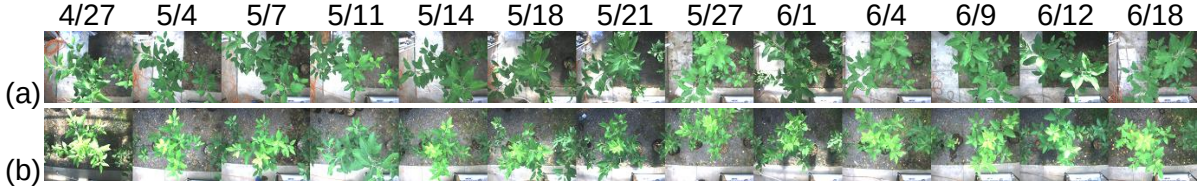

Figure 9. Canopy growth in top-view in sequence of 13 measurements from April 27 to June 18 on young apple trees with five different water treatments: (a) 100%, (b) 90%, (c) 75%, (d) 60%, and (e) 45%.

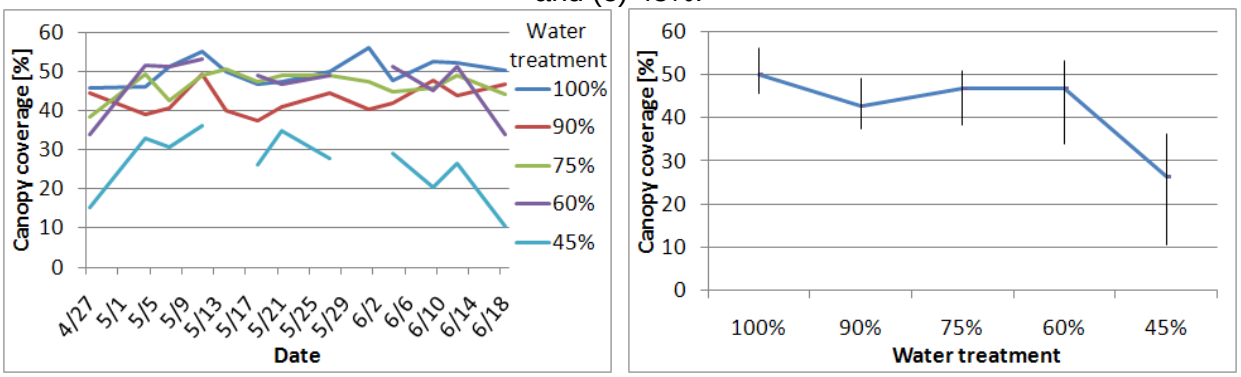

(a) (b)

Figure 10. Percentage canopy coverage to different water treatments (a) measurements along the plant growth from April 27 to June 18 (partly missing data in 60%- and 45%-watered trees lost due to an image formation problem), (b) average canopy coverage to water treatments with correlation of r = 0.7.

Conclusion

Reflectance differences between stressed and non-stressed apple trees were found based on images taken with a hyperspectral camera, even when no symptoms were present to the human eyes. No significant differences in reflectance were found in 100%-, 90%- and 75%-watered trees, suggesting all three groups are non-stressed. However, the 60%- and 45%-watered trees showed similar reflectance changes caused by water stress. Such results were also observed in monitoring soil moisture status. Among 13 spectral indices that use wavelengths within 400 – 1000 nm spectrum, Red Edge NDVI (r^2 = 0.89) within the group of narrowband indices and NDVI (r^2 = 0.68) within the group of broadband indices were highly correlated to water stress. An active spectral NDVI sensor was able to identify the spectral signature of the leaves of water stressed trees, and the performance can be improved by filtering data for valid readings. Canopy coverage obtained by a digital camera is another indicator of plant stress and identified growth changes affected by plant stress. A multispectral camera is also an alternative source for low cost and fast image capture and process as long as the selected wavelengths fit the purpose of applications. Decision support that combines multi-modal sensory data is a next step to improve plant stress detection and identify causes of the stress.

Acknowledgements

This work was supported by the US Department of Agriculture under the Specialty Crop Research Initiative, award number 2008-51180-04876.

References

Champagne, C., E. Pattey, A. Bannari, and I.B. Stratchan, 2001. Mapping crop water status: issues of scale in the detection of crop water stress using hyperspectral indices. Proceedings of the 8th International Symposium on Physical Measurements and Signatures in Remote Sensing, Aussois, France. pp.79-84.

Fredericksen T.S. and J.M. Skelly. 1994. Relation of visible and physiological ozone injury in two eastern hardwood tree species. *Phytopathology* 84:1371.

Gamon, J.A., L. Serrano, and J.S. Surfus, 1997. The Photochemical Reflectance Index: an optical indicator of photosynthetic radiation use efficiency across species, functional types and nutrient levels. *Oecologia* 112(4):492-501.

Gitelson, A.A. and M.N. Merzlyak, 1994. Spectral reflectance changes associated with autumn senescence of Aesculus hippocastanum L. and Acer platanoides L. leaves. Spectral features and relation to chlorophyll estimation. *Journal of Plant Physiology* 143(3):286-292.

Nilsson, H. 1995. Remote sensing and image analysis in plant pathology. *Annual Review of Phytopathology* 15:489-527.

Nutter F.W. Jr. and P.M. Schultz. 1995. Improving the accuracy and precision of disease assessments: selection of methods and use of computer-aided training programs. *Canadian Journal of Plant Pathology* 17(2):174-184.

Penuelas, J., I. Filella, C. Biel, L. Serrano, and R. Save, 1995. The reflectance at the 950-970 region as an indicator of plant water status. *International Journal of Remote Sensing* 14(10):1887-1905.

Potato Explorer. 2010. Leaf area index. Available at: www.potato.nl/explorer/pagina/leafarea.htm. Accessed 20 April 2010.

Sherwood R.T., C.C. Berg, M.R. Hoover, and K.E. Zeiders. 1983. Illusions in visual assessment of Stagonospora leaf spot of orchardgrass. *Phytopathology* 73:173-177.

Shokes F.M., R.D. Berger, D.H. Smith, and J.M. Rasp. 1987. Reliability of disease assessment procedures: A case study with late leafspot of peanut. *Oleagineux* 42:245-251.

Sims, D.A. and J.A. Gamon, 2002. Relationships between leaf pigment content and spectral reflectance across a wide range of species, leaf structures and developmental stages. *Remote Sensing of Environment* 81(2):337-354.

Suárez L., P.J. Zarco-Tejada, G. Sepulcre-Cantó, O. Pérez-Priego, J.R. Miller, J.C. Jiménez-Muñoz, and J. Sobrino. 2008. Assessing canopy PRI for water stress detection with diurnal airborne imagery. *Remote Sensing of Environment* 112:560–575.

Weber G.E. and E. Jorg. 1991. Errors in disease assessment-A survey. *Phytopathology* 81(10):1238.